**Response to Reviewer 1 comments**

We thank the reviewer for her/his comments, and have carefully addressed each comment and improved the paper. Below find our point-by-point responses to reviewer 1 comments, where first the reviewer comment is repeated in italics, followed by our response in bold.

Comments to the Author:

*1. Suggest describing briefly the major conclusions how aerosol size, composition and refractive index influence optical response in the abstract.*

**We have substantially rewritten the abstract to address this suggestion.**

*2. Abstract, line 13 – 15, rephrase. It is difficult to read.*

**This sentence was completely rewritten as described above.**

*3. Page 2, second paragraph, suggest adding some discussions on vertical measurement to highlight the advantage of portable scattering instruments.*

**Thanks for this comment. We added one sentence to describe advantage of portable scattering instruments for vertical profile measurements.**

*4. Page 4, line 2, make sure the density of PSL. It is 1.05 g cm-3.*

**The 1.65 g cm$^{-3}$ is the value used in the OPC-N2 software for transferring the volume concentration of ambient aerosol to mass concentration, and it is not the density of PSL.**

*5. Page 5, line 7, any reasons for choosing these four different compounds?*

**Compounds were chosen that first of all were available to us in our laboratory. More importantly, these compounds represented some of the major chemical species types (sulfate, nitrate, ammonium, organics) that we observed in the northeast US. Third, the compounds were water soluble and relatively stable, so that we could generate well characterized pure synthetic aerosols.**

*6. Use log scale for x-axis in Figure S3.*

**Thanks for this comment. As you suggestion, we modified the figure S3.**

Again thank you for all your valuable comments, which have helped to improve the paper.

Jie Zhang, Joseph P. Marto, James J. Schwab

**Response to Reviewer 2 comments**

We thank the reviewer for her/his comments, and have carefully addressed each comment and improved the paper. Below find our point by point responses, where first the reviewer 2 comment is repeated in italics, and is followed by our response in bold.

Comments to the Author:

**General comments:**

*Considering the paper focuses on an evaluation of several sensors I think much more detail regarding the sensors should be provided. For example, sample flow rates, whether or not a sheath flow is used, lower and upper concentration limits, etc. Additional information on how exactly are calibrations performed by manufacturer should be included as well.*

**Thanks for this comment. We have added the more detailed description of the sensors into the text in section 2.1, as well as updated the information of the calibration aerosol for these instruments.**

*PSL is one of the primary test particle types, but in my experience it can be very difficult generating a pure monodisperse size distribution from PSL without first passing it through a DMA. When PSL is atomized/nebulized it can produce a large mode of fine particles with sizes < 200 nm, which arises from surfactant and other contaminants in the PSL solution. These smaller particles can affect mass measurements depending on the lower detection limit of the sensor. Do the authors have any SMPS measurements showing the quality of the PSL output and confirming that it was limited to just the PSL at the expected diameters?*

**You are right and the issue is known to the authors. During our test, there were a large mode of fine particles with number size < 100nm, as shown in Figure 1a (304nm PSL for example). Fortunately the volume concentration distribution mainly concentrated around 304nm (Fig 1b). For the DRX (with the shorter wavelength light source) , the Mie calculation result of the full volume distribution is only about 6% different than the calculation using only the 304 nm PSL. Based on this calculation, we used the simplification of only considering the factory size value of PSL for our Mie scattering calculation.**

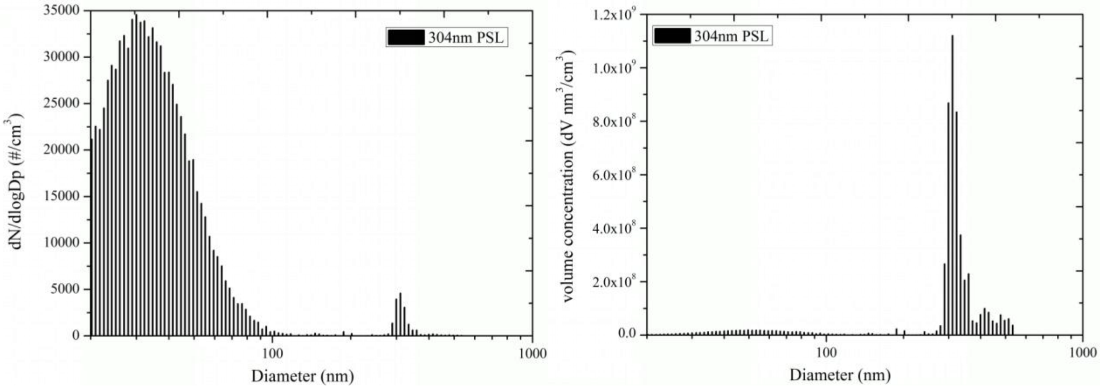

**Figure 1. Left: One sample of the lognormal number concentration distribution of 304nm PSL; Right: the volume concentration distribution of the 304nm PSL.**

*Tests were only performed on dry aerosol, which is probably necessary to eliminate the complications introduced by water uptake on particles. The manuscript would benefit from some discussion of this however, in that low-cost sensors will need to either account for RH impacts or be actively dried when sampling.*

**Thank you for this good suggestion. Actually, during lab measurements, the RH detected by PDR is below than 10%, and during ambient measurements, a silica dryer was used for keeping the RH below 40%, which is required by AMS. Based on the fact that our tests only focused on dry aerosol, we add the shortcoming of the result in the final paragraph of the conclusion.**

*Finally, I think the manuscript is significantly weakened by the lack of a true reference measurement for the ambient measurements, having to rely instead on AMS and SMPS measurements, neither of which is a true mass measurement. The authors's give a reason for this, however I find it somewhat puzzling that the TEOM was unable to provide quality measurements of ambient PM mass.*

**Actually, we had the TEOM ambient aerosol mass concentration from 12/22/2016 to 01/07/2017. Its relationship with AMS 1-hour data is shown in below Figure 2 (a) and (b). Figure 2(a) shows similar trends for TEOM and AMS, and at the same time, there is only fair ($R^2$ of 0.41 and a slope of 0.88). From figure (a), our TEOM showed higher noise than the AMS (and the other instruments), and the possible reasons maybe the flow tube which connect the TEOM to the aerosol inlet is too long. At the same time, AMS and SMPS were self-verified through estimating the aerosol density (which is needed by the SMPS) through AMS compounds measurements (Qi et al., 2005). Also our TEOM did not work from 09/27/2017 to 10/01/2017. More importantly is the very good association of the DRX, PDR, SMPS, and AMS shown in Figure 4. Clearly the TEOM is the "odd man out" in this array of measurements. Had the TEOM measurements been better quality, we would**

**have happily used them as our reference for the ambient data. Based on the above consideration, we used AMS and SMPS as reference instruments.**

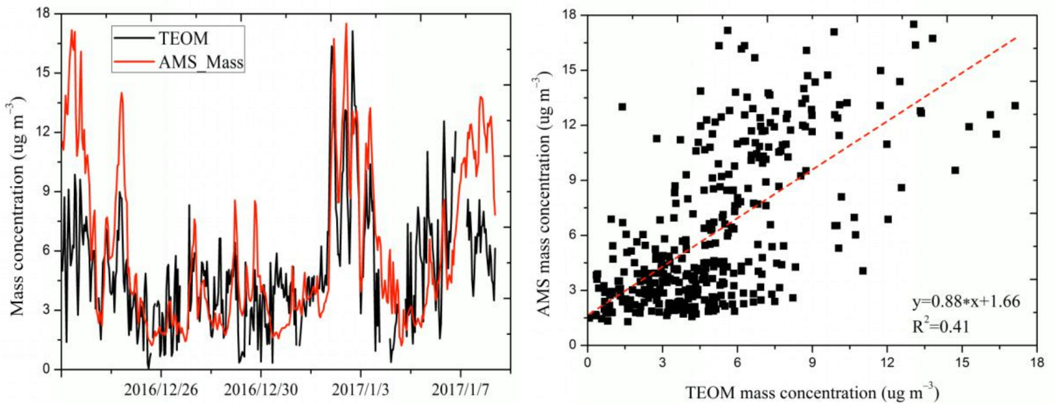

**(a)** **(b)**

**Figure 2. (a): The time series of 1-hour aerosol concentration of TEOM and AMS from 12/22/2016 to 01/07/2017 and 09/27/2017; (b) the comparison of the 1-hr PM2.5 average concentration between TEOM and AMS**

**Specific comments:**

*2, 18: recommend including a statement that the PAS is also an optical particle counter and not a direct mass measurement*

**Thank you for this comment. We had added this information into the text.**

*2, 20: there are several additional, but quite new references that could be included and compared to here, such as Crilley et al. (2018) and a paper currently in discussion (Feinbeg et al., 2018).*

**Thank you for this comment. We had added these references into the text.**

*3, 4-5: change to "aerosol mobility diameter" and to "non-refractory chemical composition"*

**Thank you for this comment. We had corrected the expression in the text.**

*3, 14 & 20: Please provide the scattering angles measured for the DRX and PDR*

**Thank you for this comment. We had added the information of the scattering angles into the text.**

*3, 25: are the specifications more specific? A D50 would be helpful if provided.*

**Thank you for this comment. We corrected the word “specifications” to “manual”. D50 data is not provided for the PDR nor the DRX. Both instruments list a “particle size range” between 0.1 and 10 microns, and this information has been added to the text.**

*4, 2: more appropriate to state that the conversion is done on volume concentrations, not number concentrations*

**Thank you for this comment. We corrected the expression in the text.**

*5, 1: please provide typical RH in the chamber for experiments*

**Thank you for this comment. We had added the information of the RH into the text (page 5, 20)**

*5, 17: While it may be true that the OPC-N2 does not measure below 380 nm, it would have still been useful to see the level of disagreement. I’m also a little surprised the TEOM could not be used due to the high-frequency noise, since this device is designed for this type of monitoring application. Could a longer averaging period have been used?*

**During the ambient measurement periods, the value of OPC-N2 was generally near to 0, so there was little point in reporting it. The problem with the TEOM is discussed above. For our TEOM, as described in the general comments section, high-frequency noise was shown, and maybe due to the flow tube which connect the TEOM and aerosol inlet was too long. Longer period would work, while short averaging period data would help us to better study the performance of DRX and PDR, so in the text, we used AMS and SMPS as reference instruments**

*7, 21: Clarify that the 0.45 g/L refer to the nebulizer solution concentration. It would be good to state the density of sucrose somewhere* ($1.59\ g / cm^3$)*.*

**Thank you for this comment. We had added the clarification into the text .**

*7, 20-22: It is strange that the OPC-N2 shows such good agreement for the sucrose in this example. It’s stated elsewhere it has a poor detection efficiency, especially below its lower limit (380 nm). Figure S3a shows aerosol volume distributions, which show at least half of the distribution below 400 nm. This would suggest the OPC-N2 misses at least half of the aerosol volume (and therefore mass), yet it looks very similar to the other two sensors, and shows good agreement with the TEOM. How is this possible?*

**Pretty much every optical sensor (and even more so for the inexpensive ones used in very low cost applications) only respond to the tail of the volume size distribution. If the shape of the size distribution is “well behaved” (or well characterized) the response can be quite linear with**

**increasing concentration. That quite well explains the OPC results. The paper takes pains to point out that when the size distribution or chemical composition is changing, one needs to take care with optical measurements.**

*The figure is also not consistent with Table 3, which lists very low ratios, as expected. Also, Figure S4's legend shows PDR * 3. Does this mean the data for that sensor are multiplied by 3? I don't think this is discussed in the text. More details should be provided justifying this if so.*

**Thank you for this comment. Table 3 illustrates that the DRX response per unit mass for the particle groups tested was consistently highest, followed by the PDR, and both are much higher than the OPC. The multiplicative factors of 3 for the PDR and 50 for the DRX reflect these relative responses, and the caption of Figure S4 is much more explicit about these factors. The main point of Figure S4 is the linearity of the responses – the measured values are in Table 3.**

*7, 23: The results suggest good linearity, but I'm not convinced on stability. Were tests repeated after some period of time, and simulated usage/exposure to ambient air? That type of test would be needed to verify stability of the response. If the author's mean stability since original calibration more details on the calibration should be given, including dates, and what was done with sensors between the time of calibration and the testing.*

**Thank you for this comment. Lab tests were repeated numerous times, always with nearly identical results. The ambient tests were performed 9 months apart, again with similar results. The optical sensors are quite stable as long as the sampled aerosol itself is stable.**

*8, 2: Is the adipic acid result normalized against the TEOM or AMS? Not clear here, but earlier it's stated the compound is too volatile to use the TEOM.*

**Thank you for this comment. The adipic acid result was normalized against the SMPS, and the statement of adipic acid calculation was stated in Page 6, 5, as well as in Table 3.**

*9, 3: The OPC-N2 provides binned results though, correct? These would have some dependence on the pulse intensity, which is related to refractive index as well as size, shape.*

**Thank you for this comment. The binned results of OPC-N2 are reported as pulse intensity, and the relationship between the calculated Mie scattering relative flux and the measurement ratio of OPC-N2 to SMPS in OPC-N2 bin range 380-540nm is shown in Figure 3. There is a linear relationship between the calculated Mie relative flux and the ratio of OPC-N2 to reference instrument (SMPS), which indicates that the OPC-N2 binned pulse intensity is related to refractive index as well as size. Based on the consideration that OPC-N2 first transfers the pulse intensity to number, then transfers**

**to mass concentration, which means that the scattering flux is not directly converted to reported the mass concentration, we did not including this result into the Mie calculation section. At the same time, we corrected our former expression in the text to ensure a more precise statement to this effect.**

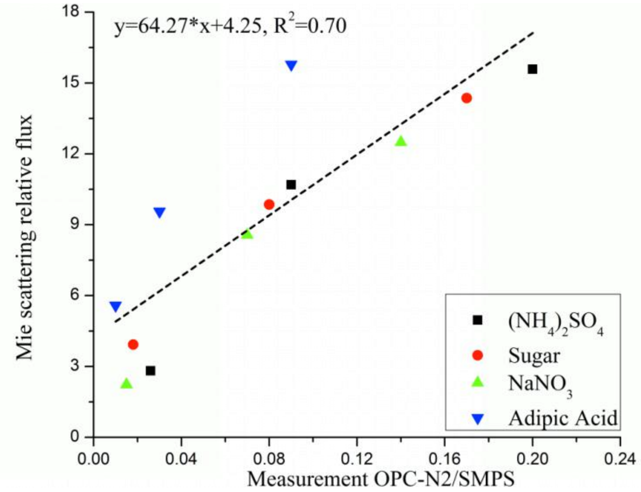

**Figure 3 The relationship of the Mie scattering relative flux and the measurement ratio of OPC-N2 to SMPS**

*9, 17: Stating this overlap range explicitly here would be helpful.*

**Thank you for this comment. We added the size range into the text.**

*9, 22: Is this section comparing number detection efficiency or mass efficiency? Please be clear.*

**Thank you for this comment. We corrected the confusing expression, and add "number" into the text.**

*10, 1-2: What is meant by this statement? The sensor response to these compounds due to the limited detection range of the OPC-N2 is poor, but that does not mean the evaluating its performance is complex.*

**Thank you for this comment. We deleted that confusing expression.**

*10, 10: Another factor not mentioned is mass from species not measured by AMS, including BC, dust, etc.*

**Thank you for this comment. During the analyzing, SMPS was lower than AMS value. Though AMS did not measure BC and dust, adding this statement would larger the difference between SMPS and AMS. So we keep the origin statement that " SMPS values ware about 15% lower than AMS,**

**which may be the result of the bias of the estimated density or the CE factor used by AMS".**

*10, 11-12: While the SMPS and AMS are consistent, I think the argument that this means the AMS is a good reference instrument for mass is somewhat weak. This is where the analysis suffers from not including the TEOM, a true PM mass reference measurement method.*

**Thank you for this comment. As noted above, a well operating TEOM with low noise would have been useful to the study. However, in addition to the reasoning above, the TEOM versus AMS measurements from numerous field and lab studies (including the lab studies presented in this paper) give us high confidence in the AMS as a good mass measurement for non-refractory submicron particles. Since this type of particle encompasses the vast majority of what we measured, we are confident in using the AMS for this purpose.**

*10, 14: This seems like a large difference between two instruments both calibrated against the same material (Arizona test dust)*

**The difference from the difference of wavelength used by these two instruments. As shown in lab tests, these two instruments show a big difference for same aerosol distribution. So though they are calibrated by same material, they can respond differently for ambient aerosols in situations with quite different size distributions. A second difference is the calibration factors used. The two instruments recommend different calibration factors for "ambient" measurements.**

*11, 1-2: This statement needs to be supported by more evidence. What constitutes "ambient aerosol" according to TSI? Why is the difference plausible? It seems like the aerosol composition at the test site is not radically different from what would be considered a regional, continental aerosol (as opposed to say, a heavily marine influenced location).*

**The calibration factor 0.38 came from Wallace's result (Wallace et. al., 2011), which tested the DRX for ambient air in one location. A complete characterization requires data for many different kinds of aerosol, including aerosol composition as well as size distribution for Wallace's study and our study. From the TSI "APPLICATION NOTE EXPMN-007", there were still different calibration factors for ambient air, and TSI mainly suggests the one from Wallace's result. For the aerosol composition from regional, continental vs. Marine location, they would be different, and new calibration factors are still needed.**

*11, 4-12: It seems like the more straight-forward way to evaluate this relationship would be to plot ratios of each sensor to the reference as a function of mass mean diameter measured by the SMPS, as shown in Figure 6. Suggest removing.*

**Thank you for this comment. After considering carefully, we think it is truly not necessary. So we deleted the whole paragraph.**

*11, 16: I suggest swapping the axes to show mean diameter on the x-axis.*

**Thank you for this comment. We use "DRX(PDR)/AMS ratio" as "x axes" to emphasize the performance of these sensors, and give readers more directly impression. We would keep the original use.**

*12, 26: where do these estimated RI come from? Are they based on the aerosol composition?*

**The refractive index is estimated based on the above method mentioned in section 3.5 using the reference table.**

*Table 1: Suggest adding rough cost of each instrument as I think it is relevant in the context of the manuscript.*

**Thank you for this comment. We had added the price information into text (Table 1).**

*Table 3: It would help reader interpret the different groups if you listed the median diameter or similar parameter under the group name. Information in Table 4 could combined here and eliminate a table.*

**Thank you for this comment. We added the median diameter below different groups, and combining Table 3 and Table 4 into one. Thank you so much!**

Again thank you for all your valuable comments, which have helped to improve the paper.

Jie Zhang, Joseph P. Marto, James J. Schwab

# Exploring the Applicability and Limitations of Selected Optical Scattering Instruments for PM Mass Measurement

Jie Zhang*, Joseph P. Marto, James J. Schwab

Atmospheric Sciences Research Center, University at Albany, State University of New York, NY, USA

*Correspondence to: Jie Zhang, Email: jzhang35@albany.edu

# Exploring the Applicability and Limitations of Selected Optical Scattering Instruments for PM Mass Measurement

Jie Zhang*, Joseph P. Marto, James J. Schwab

Atmospheric Sciences Research Center, University at Albany, State University of New York, NY, USA

*Correspondence to: Jie Zhang, Email: jzhang35@albany.edu

**Abstract:** Two optical scattering instruments for particle mass measurement - the Thermo Personal Data RAM (PDR-1500), the TSI Environmental DustTrak DRX (Model 8543) were evaluated by 1) using poly- and mono-disperse test aerosol in the laboratory, and 2) sampling ambient aerosol. The responses of these optical scattering instruments to different particle characteristics (size, composition, concentration) were compared with responses from reference instruments. A Mie scattering calculation was used to explain the dependence of the optical instruments' response to aerosol size and composition. Concurrently, the detection efficiency of one Alphasense Optical Particle Counter (OPC-N2) was evaluated in the laboratory as well. The relationship between aerosol mass concentration and optical scattering was determined to be strongly dependent on aerosol size, and to a lesser extent on aerosol composition (as reflected in the refractive indices of the materials tested) based on ambient measurements. This confirms that there is no simple way to use optical scattering instruments over a wide range of conditions without adjustments based on knowledge of aerosol size and composition. In particular, a test period measuring ambient aerosol with optical scattering instruments and a mass based method (an Aerodyne Aerosol Mass Spectrometer) determined that roughly two thirds of the variance ($R^2 = 0.64$) of the optical to mass signal ratio is explained by the aerosol mass median diameter alone. These observations and calculations help evaluate the applicability and limitations of these optical scattering instruments, and provide guidance to designing suitable applications for each instrument by considering aerosol sources and aerosol size.

## 1 Introduction

The measured mass concentration of fine particulate matter (PM2.5) both indoors and outdoors is important for many reasons (Chow et al., 2005; McMurry, 2000; Bae et al., 2010; Brauer et al. 2011). A major reason is that fine particulate matter is associated with adverse effects on human health, specifically increased morbidity and mortality rates (Dockery et al., 1993; Landen et al., 2011). The standard mass concentration measurement method established by the U.S. Environmental Protection Agency (EPA) for compliance with National Ambient Air Quality Standards (NAAQS) is based on gravimetric filter sampling and weighing (Sousan et al., 2016a), which are repeatable and have well-characterized accuracy and precision. However, these methods cannot provide real-time aerosol mass concentration, which limits the information available regarding aerosol sources, diurnal variation (Wallace et al., 2011), and high concentration spikes of short duration (Chung et al., 2001).

These drawbacks can be avoided by using real-time continuous instruments, most commonly the Tapered Element Oscillating Microbalances (TEOM) or Beta Attenuation Monitors (BAM) (EPA, 2013). However, due to the high cost and large size of these instruments, it is difficult to deploy these real-time instruments for quick-response situations or in a wide spatial coverage, especially in remote areas and developing countries. Less expensive, portable, small sensors which use light scattering to infer particle mass concentration have become available in the past few decade, and they are currently drawing much attention as an alternative to the well-established methods described above (Hinds et al., 1999; Holstius et al., 2014; Wang et al., 2015; Wang et al., 2016). These portable sensors can provide high time resolution real time data, be deployed in dense networks at reasonable costs, and also they are suitable for vertical aerosol profile measurement lunched on small balloon or aircraft (Mamali et al., 2017).

Typically, these light scattering sensors are calibrated by the manufacturer using a specific test aerosol, which may or may not be representative of ambient testing conditions at a given location. For this reason, there is ongoing interest in evaluating the capabilities and limitations of optical scattering sensors in the laboratory when challenged with aerosol of varying sizes and compositions (Crilley et al., 2018; Holstius et al., 2014; Li and Biswas, 2014; Sousan et al., 2016a; Wallace et al., 2011; Wang et al., 2015). Sousan et al. (2016b) found the OPC-N2 (Alphasense Ltd) performed similarly to the PAS-1.108 (Portable Aerosol Spectrometer, GRIMM 2010, also an optical particle counter) for particles with diameter above 1 µm. In other studies, laboratory measurements were complemented by field comparisons with reference instruments (such as

TEOM or gravimetric filter methods). Wallace et al. (2011) suggested a calibration factor of 0.38 for the DustTrak when sampling ambient aerosol after comparing the instrument with TEOM data. Crilley et al. (2018) evaluated the performance of OPC-N2 for ambient measurements in UK, and a reasonable agreement was found comparing to reference instruments. Feinberg et al. (2018) shows high correlations between optical PM sensors (such as AirCasting AirBeam, Shinyei PMS-SYS-1 etc.) and reference monitors in Denver, Colorado, USA.

Investigating the fundamental performance of these optical instruments for different kinds of aerosol aids in understanding their properties and guiding their suitable use. Based on these considerations, experiments were designed and performed to evaluate three distinct optical sensors - the Thermo Personal DataRAM (PDR-1500), the TSI Environmental DustTrak DRX (Model 8543), and the Alphasense Optical Counter (OPC-N2) - using mono-disperse aerosol to study the instrument's dependence on particle size, and poly-disperse test aerosol to study the effect of aerosol refractive index (related to chemical composition). A Mie scattering calculation was used to quantitatively describe the performance of these instruments. Optical instruments readings were then related to the aerosol mobility diameter measured by Scanning Mobility Particle Sizer (SMPS) and chemical composition of non-refractory ambient aerosol measured by a High Resolution Time-of-Flight Aerosol Mass Spectrometer (HR-TOF-AMS) to provide detailed analysis of the effects of ambient size and chemical composition on the response of these optical instruments. Using these laboratory results, the average refractive index of the ambient aerosol was estimated based on the response of optical instruments and the aerosol size distribution.

## 2 Methods

### 2.1 Instrumentation

The TSI DustTrak DRX (model 8543, hereafter DRX) is a combined photometer and optical counter, which uses a 655 nm laser to illuminate a sample stream and measures the intensity of scattered light perpendicular to the stream with a photodetector (Wang et al., 2009; TSI Inc., 2017). Its scattering angle is 90°. The measured intensity is a function of the total particle volume, the particle refractive index, and the particle shape (Wallace et al., 2011). The measurable mass range (software determined) is 0.001 to 150 mg $m^{-3}$, and size range is 0.1 to 10 um. Scattering intensities of individual particles are used to group particles into broad size bins - typically $PM_1$, $PM_{2.5}$, $PM_4$, and $PM_{10}$. The total flow rate of the DRX was set to 3 LPM, with 2 LPM of this total flow as measured aerosol sample flow, while the other 1 LPM is filtered and used as sheath flow (TSI Inc., 2017). The DRX is calibrated by TSI using ISO 12103-1, A1 Arizona test dust. The default calibration factor of 1 was used for this study.

The PDR-1500 (Thermo Fisher Scientific Inc., 2014, herafter PDR) is a highly sensitive nephelometric monitor using an 880 nm wavelength LED source for particle scattering measurement. Its forward scattering angle covers 60° to 80°. The measurable mass range of PDR is 0.001 to 400 mg $m^{-3}$, and its size range is 0.1 to 10 um. During the measurement, the flow rate of PDR is set to 1.5 LPM. The PDR-1500 was factory calibrated against a gravimetric standard traceable to the National Institute of Standards and Testing (NIST) by the manufacturer using SAE Fine (ISO Fine) supplied by Powder Technology, Inc..

The OPC-N2 (Alphasense Ltd., 2015, hereafter OPC-N2) measures the intensity of light scattered from particles using an optical receiver at a forward angle of approximately 30° (Sousan et al., 2016b). The light intensities are binned and reported as particle counts in 16 size bins from 380 nm to 17 µm. The laser wavelength of OPC-N2 is 658 nm, and the total flow rate is 1.2 LPM, of which 0.22 LPM is used for the aerosol measurements. The maximum particle count rate is 10000 particle/second. The number and sizing of the OPC-N2 were calibrated by the manufacturer using polystyrene latex (PSL) particles, and for ambient measurements a constant density of 1.65 g $cm^{-3}$ is used for converting the volume concentration to mass concentration.

Our reference instruments included a TSI Scanning Mobility Particle Sizer (SMPS), which consisted of an Electrostatic Classifier (EC, model 3080), a Differential Mobility Analyzer (DMA, model 3081), and a Condensation Particle Counter (CPC, model 3785). The SMPS operated with a 10:1 sheath-to-sample flow ratio (sheath flow 3 L $min^{-1}$, and sample flow 0.3 L $min^{-1}$), which led to an effective measured aerosol mobility size range of 14.9 nm to 673.2 nm. A tapered element oscillating microbalance (TEOM) mass monitor (R&P Model 1400ab), provided continuous gravimetric-based non-volatile aerosol mass concentrations with a time resolution of 5 mins (Hogrefe et al., 2004). An Aerodyne HR-TOF-AMS (hereafter AMS) was also used to measure the chemical composition and mass size distributions of selected species in real-time for non-refractory sub-micron aerosol (Drewnick et al., 2005; Sun et al., 2012). A collection efficiency (CE) factor of 0.5 was used to account for the aerosol loss caused by aerosol bounce at the vaporizer and aerosol lens transmission (Zhang et al., 2005, Canagaratna et al., 2007, Sun et al., 2009, 2011). The default relative ionization efficiencies (RIE) of organic compounds (1.4), nitrate (1.1), sulfate (1.2), ammonium (4), and chloride (1.3) were used (Jimenez et al., 2003; Lee et al., 2016). Aerosol density was determined from AMS measurements of the weighted contributions of major chemical species to the total mass concentration, as described in the Supplement.

## 2.2 Experimental setup

The experiments were conducted first as a laboratory evaluation, which evaluated the performance of optical sensors under controlled aerosol conditions, and second as ambient tests, which evaluated the performance of sensors under ambient aerosol conditions, including the effect of aerosol size and composition on sensor readings.

The laboratory setup used for evaluation and calibration of optical instruments has been described by Hogrefe et al. (2004) and is shown in Fig. 1. The laboratory system consisted of an aerosol generation and dilution system, as well as a 500-liter aerosol chamber with sampling ports. The aerosol generation instrument was a constant output atomizer (TSI Model 3076). The dilution system reduced the aerosol mass concentration produced by the atomizer and dried the aerosol using dry air flow (generally below 10% RH, measured by PDR). Before sampling by the different instruments, the generated aerosol underwent equilibration in the aerosol chamber. The instruments sampled from the middle of the chamber, and about 20 minutes was required for the instruments to stabilize after each modification to the dilution or generation system. For evaluating the dependence of optical sensor performance on size, different-sized, mono-disperse PSL particles were used. For each size PSL, dilution liquid was incrementally added during measurement to vary concentration. After the PSL experiments, synthetic particles with four different chemical compositions ($NaNO_3$, $(NH_4)_2SO_4$, sucrose, adipic acid) were generated for testing the performance dependence on particle composition, as light scattering is affected by particle refractive index (Seinfeld and Pandis, 2016). For each material, the solution concentration and/or the amount of dilution air was varied during experiments to modify the concentration.

During these experiments, the TEOM was used as the reference instrument for $NaNO_3$, $(NH_4)_2SO_4$, sucrose, and PSL particles because it had the same sampling location as optical instruments. The SMPS was used as the reference for adipic acid, due to adipic acid's high volatility (Mønster et al., 2004; Seinfeld and Pandis, 2016) and observed loss on the 50° C TEOM mass sensor.

For ambient experiments, two optical sensors (DRX and PDR), one HR-TOF-AMS, and one SMPS were connected to a dryer, to keep the RH below 40%, and then connected to outside air through a vent port. The OPC-N2 was not used for these tests due to its size detection limit (380 nm) being larger than the most ambient aerosol of this study, while TEOM is not used due to its high frequency noise in ambient measurement.

### 2.3 Mie scattering calculation

The Mie scattering calculation followed the techniques in the MATLAB version of Mie theory for homogeneous spheres described by Mätzler (Mätzler, 2002). The required input parameters include the complex refractive index, the sphere radius, light wavelength, and the scattering angle (Li and Biswas, 2017). Considering only spherical particles is reasonable in our situation because smaller non-spherical particles (< 1um) are more similar to their spherical phase than larger ones (Smith, 2009). The scattering angles and light wavelengths used in these three optical instruments are listed in Table 1, and the scattering angle of 90 degrees for the PDR was used for simplicity. Using scattering angles between 60° and 80° will change some details of the scattered flux, but the linearity of the scattered flux with aerosol amount will not be affected. Combining these sensor and aerosol parameters, the relative scattering flux per unit aerosol volume (RF_v) for each particle size was then calculated. Knowing the normalized volume distribution (NVD) of the generated aerosol, the integrated relative flux (hereafter RF) expected to be received by the sensor detector was estimated by summing the product of RF_v and NVD over the whole particle size distribution. RF was then used to evaluate the performance of optical instruments and for comparison to measured mass concentrations.

## 3 Results and discussion

### 3.1 Performance for mono-disperse particles

The dependence of DRX, PDR, and OPC-N2 performance on particle size was studied using five sizes (90±14 nm, 173±9 nm, 304±9 nm, 490±15nm, and 1030±31 nm) of PSL particles (Ted Pella, Inc.). To compare optical sensors with the reference instrument (TEOM), 15 minutes of data collected at the end of each mass concentration plateau were averaged.

The relative responses of the optical sensors (PDR, DRX, and OPC-N2) compared to the TEOM for the mono-dispersed PSL particles are shown in Table 2. The outputs of these sensors were linearly regressed against particle mass concentration measured by the TEOM to get the ratio of optical sensor response to TEOM readings, and all results were well-correlated ($R^2$>0.90). The results from the PDR and DRX for 304 nm PSL particles are shown in Fig. S1 as an example. As particle size increased in these experiments, the responses of the PDR and DRX showed a maximum for one specific size PSL (304 nm for DRX, and 490 nm for PDR). For both instruments, these sizes were closest to half of the light source wavelength used by the sensor. For OPC-N2, this maximum was missed due to its lower detection limit of 380 nm. For PSLs large enough to trigger a response, the OPC-N2 detection efficiency was still lower than 1 for these two sizes – the detection efficiency was 68% for 490 nm and only 48% for 1030 nm.

Mie scattering calculation results were used to explain the observed performance characteristics of the DRX and the PDR. The relative scattering fluxes from particles for conditions appropriate to the DRX and PDR are shown in Fig. S2 and Table 2. Figure S2a shows that the RF peaks at about 400 nm for DRX and 550 nm for PDR, which matches the results shown in Table 2, and as particle size increased beyond peak size, the relative scattering flux decreased. High correlation coefficients were obtained for regressions of RF versus the optical instrument-to-TEOM signal ratio, with $R^2$=0.97 for DRX and 0.81 for PDR as shown in Fig. S2b. This is indicative of the general positive relation between the calculated RF with optical instrument's response to

PSL. The values for 90 nm PSL are not used in this analysis, since both the DRX and PDR showed high response bias for 90nm PSLs, which may be caused by the proximity of 90 nm to their detectors' size limits (100n m for DRX and PDR, Thermo Fisher Scientific Inc., 2014; TSI Inc., 2017), the uncertainty introduced by using a single scattering angle in the calculation, and/or the "non-PSL" very small aerosol generated when atomizing the PSL containing solution.

## 3.2 Performance for poly-disperse particles

### 3.2.1 Mass concentration dependence on particle composition

To focus on the instruments' dependence on particle composition (mainly the effect of refractive index), three groups of tests with different concentration liquid samples were performed, and are shown in Table S1. The changes in solution concentration produced a shift in aerosol number/mass size distribution sampled by the instruments. In each of the three groups, concentrations were selected such that the volume size distributions of the four compounds were very similar (as shown in Fig. S3).

The ratios of readings from the optical instruments to those of the reference instruments for different kinds of aerosol in each group were determined, and are shown in Table 3. A strong, linear relationship between the DRX, PDR, and OPC-N2 with the TEOM for 0.45 g $L^{-1}$ (atomizer solution concentration) sucrose (density 1.59 g $cm^{-1}$) was found, with $R^2$=0.99 for all three optical sensors, as shown in Fig. S4 as an example. For the other groups of particles and concentrations tested, the results were similar. This illustrates the high linearity of the responses of these optical instruments when challenged with pure substances of a stable particle size distribution.

Table 3 shows the variation of optical to mass ratios related to the aerosol composition in each group, in addition to an inter-comparison between different groups. For low dilution concentrations (Group 1), the DRX showed a higher response (ratio vs TEOM) for sucrose (slope=0.92), and $(NH_4)_2SO_4$ (slope=0.85), but lower ratios for $NaNO_3$ and adipic acid (58% and 61%, respectively). Similar performance was also shown for the PDR and OPC-N2. A lower detection ratio was observed for the OPC-N2, due to its detection limit (380 nm), as it would fail to detect many particles. Ratios of optical to mass signals for different particles are also related to their refractive index, and the aerosol with a larger refractive index results in a higher measurement ratio. More detailed discussion will be given in the next section, and the refractive indices of these materials are shown in Table 3 (Weast, 1976; Seinfeld and Pandis, 2016). For moderate and high concentrations, similar behavior was observed. Generally, the DRX and PDR produced higher optical to mass signal ratios for particles with larger refractive indices. It is worth noting that only bright aerosols were tested, meaning that the imaginary part of the refractive index of the aerosol was zero.

Since the median diameter of the volume size distributions increased from Group 1 to Group 3 as seen in Table S1, the increase in optical response shown in Table 3 verifies the size dependence illustrated by the PSL and presented in the previous section. That is, the response ratios of the optical instruments increase with increasing particle size for the same particle material in these three groups. Also, with increasing particle size, the difference between DRX and PDR decreased from about 2.7 times for the smallest median diameter, to 1.7 times for the largest median diameter. With size distribution shifting to larger sizes, the PDR displayed a larger relative response (to the TEOM) due to its longer wavelength light source.

### 3.2.2 Mie scattering calculation for optical instruments

For Mie scattering calculations, all particles were assumed to be spherical, and their refractive index was independent of wavelength over the range of interest. Refractive indices of the four materials are shown in Table 3. Some materials have two or three different refractive indices, the values of which are related to their crystal structure (Eggleton et al., 1991). To account for this effect, the relative scattering flux was calculated by using the maximum and minimum refractive indices, which produced a range of relative flux values for the material. The maximum and minimum relative fluxes were then averaged to represent a best estimate relative scattering flux of the material, and the difference between averaged value and minimum value was used as the error range. Following the above method, the relative Mie scattering flux of these four particle compounds was obtained for the optical sensors at different dilution concentrations as shown in Table S2. Here the Mie relative flux was only calculated for the DRX and PDR, and not the OPC-N2. This is because the DRX and PDR responses are directly related to the scattering flux, while the OPC-N2 response is directly related to the estimated aerosol number concentration - though its measured binned pulse is related to aerosol refractive index and aerosol size.

The highly correlated relationship of the Mie scattering relative flux and the measurement ratios of DRX and PDR to TEOM ($R^2$=0.95 for DRX and 0.90 for PDR) shown in Fig. 2, verifies the linear relationship between RF and the ratio of optical to mass signals for this study, and provides an explanation of the performance of DRX and PDR for the variation in particle composition and size. The particle with a higher refractive index (such as $(NH4)_2SO_4$ and sucrose) or larger size distribution, produces a larger relative flux for optical instruments, resulting in higher instrument response and subsequently a higher measurement ratio of optical sensor readings to reference values.

### 3.3 Detection efficiency of OPC-N2

To evaluate the counting ability of OPC-N2 in more detail, the detection efficiency in the first size range channel (380-540 nm) of the OPC-N2 was analyzed. The limited size range was determined using the overlap of SMPS size range (14.9-673.2 nm) with OPC (detection limit of 380 nm). Using the measurements from the OPC and SMPS size distributions, the particle number counts of these two instruments were calculated in the overlapping size range (380-540 nm), in units of number per $cm^3$. The comparison of OPC-N2 and SMPS measurement values is shown in Fig. 3. In the analysis, $(NH_4)_2SO_4$ readings showed saturation when OPC counts were higher than 300 $cm^{-3}$. Excluding the saturated data, all four compounds ($(NH_4)_2SO_4$, $NaNO_3$, sucrose, adipic acid) displayed strong linear relationships between SMPS and OPC-N2 counts, with all $R^2$ >=0.99.

As with the DRX and PDR, the number detection efficiency of the OPC-N2 showed substantial differences with aerosol composition. For $NaNO_3$, the OPC-N2 number detection efficiency was as high as 103% when compared to the SMPS. However, it was only 42% for $(NH_4)_2SO_4$, 55% for sucrose, and 16% for adipic acid. The low number detection efficiency of the OPC-N2 for many of these compounds helps explain the low ratio of the OPC to SMPS in Table 3.

### 3.4 Ambient measurement

Ambient measurements were recorded from 12/22/2016 to 01/07/2017, and from 09/27/2017 to 10/01/2017 to study the performance of PDR and DRX under ambient aerosol conditions. The time series of 1-hour aerosol concentration readings of the DRX, PDR, AMS, SMPS are shown in Fig. 4, and the aerosol chemical species mass concentrations and mass fractions are shown in Fig. S5.

Figure 4 shows very similar behavior (that is, high and low excursions) for the DRX, PDR, SMPS, and AMS measurements. AMS measurements showed high correlation ($R^2$=0.94) with SMPS mass concentration, and the regression slope = 0.85 as shown in Fig. S6a. The 15% difference between the AMS and SMPS may be the result of the bias of the estimated aerosol density or the CE factor used by AMS. The high correlation verifies the performance of AMS for these periods and its reliability as a reference instrument. The even higher coefficient of determination ($R^2$=0.96) between the PDR and the DRX (Fig. S6b) shows the comparability of these two optical instruments, and the slope of 1.81 is due to the different factory calibration factors for the instruments. Of all the DRX vs PDR data in Fig. S6b, there was one set of data points clearly deviating from the main cluster, and these data points came from 9/28/2017 02:00 to the end of this study. At that date and time, a cold front passed through Albany, causing aerosol mass concentration to drop quickly, from about 11 ug $m^{-3}$ to 2 ug $m^{-3}$, and aerosol mass median diameter (measured by SMPS) dropped from 280nm to 200nm while the organic compound fraction increased to above 80%, as shown in Fig. S5. This deviation shows the influence of aerosol characteristics (mainly aerosol size here) on the optical instruments. The comparisons between the optical instruments with AMS are shown in Fig. 5. The PDR data shows a little more scatter than the DRX data ($R^2$ 0.86 vs. 0.91), and the slope of PDR to AMS was 1.03 (near to 1), while the slope of DRX to AMS was 1.96, indicating a calibration factor of 0.52 for the DRX would be appropriate for this data. This calibration factor is higher than thatr recommended by the manufacturer for ambient aerosol (0.38, TSI Inc., 2017; Wallace et al., 2011). This difference in recommended calibration factor based on aerosol size and composition is an important result and deserves to be widely recognized.

The combination of aerosol median diameter, aerosol chemical mass fractions, and the ratio of optical instrument values to AMS mass concentrations can be used to verify the above assumption that the aerosol size is the most important variable in this study. Plots combining these parameters are shown in Fig. 6 (PDR) and Fig. S7 (DRX). Figure 6 shows the correlation scatterplot of aerosol median diameter plotted versus the PDR/AMS ratio. All points are color-coded by organic mass fraction, and sized by AMS mass concentration. A moderate coefficient of determination ($R^2$=0.64) with positive slope indicates the clear relationship between mass median diameter and PDR/AMS ratio. The random distribution of organic-rich (red) points and inorganic-rich (blue) points in Fig. 6 and Fig. S7 suggests aerosol composition has a smaller effect on the response of these optical instruments. For example, the organic mass fraction corresponding to DRX/AMS ratio = 1 ranged from 0.3 to 0.8 in Fig. S7. Figure 6 does show clustered organic-rich particles in the smaller size range (lower left points), as well as inorganic-rich particles in the large size range (upper right points). A likely reason for this is that the small size range particles were newly-emitted fresh aerosol that was characterized by very high organic fraction, small-size distribution and externally- mixed properties (note that organics had a small second peak at about 150nm, Fig. S8a, Sun et al., 2009), while the large particles were related to aged regionally representative aerosol, characterized by higher $SO_4$ mass fraction, large-size organic/$SO_4$ mass distribution as well as internally-mixed properties (both peak about 400 nm, Fig. 8b, Sun et al., 2009).

The dependence of the optical sensors on aerosol size highlights an important consideration for the use of optical scattering sensors in critical applications. It is clear that different correction factors should be used in different measurement conditions instead of a single constant value (McNamara et al., 2011). For example, the PDR, when used in a rural forest environment with high concentrations of fresh organic-rich small size aerosol, the response ratio may be as high as 2.50 based on the results of this study, while for an area which would be strongly impacted by aerosol transported long distances, such as the northern U.S. regions affected by long-range transported wood-fire produced aerosol from western Canada (Le et al., 2014) or biomass-burning aerosol from of the central U.S. (such as the Mississippi Valley, Zhang et al., 2008), the correction factor could be as low as 0.60. These lowest response ratios might be expected when Albany was affected by biomass-burning aerosol from southern Mississippi Valley as shown in Fig. S9.

### 3.5 Ambient aerosol refractive index estimation

Assuming the relationship between RF and the ratio of optical instruments to reference instruments is constant for lab tests of pure composition aerosols (Fig.2) and ambient aerosol, the average ambient aerosol refractive index real part can be derived. The averaged RF of optical instruments is calculated based on that linear relationship and the ratio of optical o AMS signals. From this a reference table of RF for different refractive indices can be built based on the normalized volume size distribution and the assumed differences in refractive index (from 1.2 to 1.8 with step of 0.01), as shown in Table S3. After comparing the calculated RF with the RF in the reference table, the refractive index of the ambient aerosol may be estimated. Figure S10 shows the estimated time series of 1-h refractive index real part using the above method based on PDR and DRX data. Generally, the relative difference between these two estimations was below 10%, with the largest discrepancy after 09/28/2017. A likely explanation of this larger difference is the smaller particles in this period biasing the optical instruments relative responses. The averaged value determined for the refractive index was 1.54 for PDR and 1.55 for DRX, which was very near to the estimated value 1.56 (Hand et al., 2002), and within the estimated range of 1.54 to 1.72 (Ebert et al., 2004). The correlation scatter plot of aerosol refractive index and the PDR/AMS ratio (Fig. S11a) verifies the smaller effect of refractive index on PDR/AMS ratio compared to aerosol size, with a similar result for the DRX (Fig. S11b). One possible reason for this is that the range of variation of refractive index of this study was relatively small (88% points in 1.48-1.58), which was not enough to cause significant variation in the optical instrument responses.

## 4 Conclusion

In this study, the performance of three optical sensors (DRX, PDR, and OPC-N2) was evaluated using 1) poly- and mono-disperse aerosol in the lab, and 2) ambient aerosol (PDR and DRX only). The aim of this evaluation was to study the applicability and limitations of each optical sensor. A Mie scattering calculation was used to describe the results of these measurements. During laboratory tests, good linear relationships (generally $R^2>0.90$) were shown between the optical measurements and the traditional mass measurements, while the slope depended on aerosol size and aerosol composition. The response of these optical instruments can be well explained by the Mie scattering calculations. During the mono-disperse particle tests, the DRX was more sensitive to smaller particles than the PDR, which is consistent with its shorter wavelength light source. During the poly-disperse particle experiments, all three sensors showed higher responses for sucrose and $(NH_4)_2SO_4$, and lower responses for $NaNO_3$ and adipic acid, which illustrates the important effect of refractive index (or particle chemical composition) on instrument performance. The aerosol with higher refractive index or larger size produced more scattering flux, and therefore a higher instrument response.

During ambient aerosol experiments, the DRX and PDR were directly compared to the reference instruments (SMPS and AMS). By exploring the aerosol mass median diameter measured by SMPS and combining the mass fraction loading of aerosol compounds measured by AMS, we found aerosol size (represented by aerosol mass median diameter) has the greatest impact on the relative optical response in this study when compared to the chemical composition of the aerosol compounds and the aerosol refractive index. The aerosol refractive index was estimated based on the relationship of RF with the ratio of optical instruments to reference instruments, the normalized volume size distribution, and a reference table.

The dependence of the optical sensors on aerosol size highlights an important consideration about aerosol size distribution in the use of optical scattering sensors. For field ambient aerosol measurements, the characteristics of aerosol sources, such as traffic emissions or forest-based new particle formation may affect on the quality of the sensor data. Knowledge of the size distributions of aerosol from former studies would help to determine more accurate calibration factors for optical instruments. However, due to the limit of SMPS measurements (upper size limit <700 nm in our case) and AMS measurements (upper size limit <1000 nm, and only detects non-refractory species), the relatively short time period of measurements in this study, and a lack of diversity of aerosol sources, more ambient measurements will be necessary to more fully map out the range of calibration factors required for the application of optical instruments. This study mainly focused on dry aerosol (the detected aerosol RH by PDR in lab is below 10%, and during ambient measurements, the dryer kept the RH below 40%), the dependence of optical instruments on RH needs further study. Despite the complexity of determining calibration factors, as well as instrument limitations, these compact optical instruments will hopefully provide increasingly reliable data covering a greater spatial extent.

Additional studies and measurements will help better characterize the aerosol, and it is hoped they will provide further accurate information that will help inform and design plans to improve ambient air quality.

Acknowledgements: This work has been supported by the New York State Energy Research and Development Authority (NYSERDA) contract number 48971. Special thanks go to research scientist Dr. Patricia Fritz (New York State Department of Health) for granting use of the PDR, Xiuli Wei and Hui Shi for helping in the lab work, and Brian Crandall for assistance with the editing of this paper.

## Reference:

Alphasense, L. (2015). User Manual: OPC-N2 Optical Particle Counter. 072–0300, Issue 3.

Bae, M. S., Schwab, J. J., Hogrefe, O., Frank, B. P., Lala, G. G., and Demerjian, K. L. Characteristics of size distributions at urban and rural locations in New York. Atmospheric Chemistry and Physics, 10(10), 4521-4535, 2010.

Brauer, M., Amann, M., Burnett, R. T., Cohen, A., Dentener, F., Ezzati, M., Henderson, S.B., Krzyzanowski, M., Martin, R.V., Van Dingenen, R., Van Donkelaar, A and Thurston, G.D. Exposure assessment for estimation of the global burden of disease attributable to outdoor air pollution. Environmental science and technology, 46(2), 652, 2011.

Canagaratna, M. R., Jayne, J. T., Jimenez, J. L., Allan, J. D., Alfarra, M. R., Zhang, Q., Onasch, T. B., Drewnick, F., Coe, H., et al. Chemical and microphysical characterization of ambient aerosols with the aerodyne aerosol mass spectrometer. Mass Spectrometry Reviews, 26(2), 185-222, 2007.

Chow, J. C., Watson, J. G., Savage, N., Solomon, C. J., Cheng, Y. S., McMurry, P. H., Corey, L.M., Bruce, G.M. Pleus, R.C., Biswas, P., and Wu C.Y. Nanoparticles and the Environment. Journal of the Air and Waste Management Association, 55(10), 1411-1417, 2005.

Chung, A., Chang, D. P., Kleeman, M. J., Perry, K. D., Cahill, T. A., Dutcher, D., McDougall, E. M., Stroud, K. Comparison of real-time instruments used to monitor airborne particulate matter. Journal of the Air and Waste Management Association, 51(1), 109-120, 2001.

Crilley, L. R., Shaw, M., Pound, R., Kramer L. J., Price, R., Young, S., Lewis, A. C., Pope, F. D. Evaluation of a low-cost optical particle counter (Alphasense OPC-N2) for ambient air monitoring. Atmospheric Measurement Techniques, 11(2): 709-720, 2018.

Dockery, D. W., Pope, C. A., Xu, X., Spengler, J. D., Ware, J. H., Fay, M. E., Ferris, B. G., and Speizer, F. E. An Association between Air Pollution and Mortality in Six U.S. Cities. New Engl. J. Med., 329:1753–1759, 1993.

Drewnick, F., Hings, S. S., DeCarlo, P., Jayne, J. T., Gonin, M., Fuhrer, K., Weimer, S., Jimenez, J. L., Demerjian, K. L., Borrmann, S., Worsnop, D. R. A new time-of-flight aerosol mass spectrometer (TOF-AMS) -Instrument description and first field deployment. Aerosol Science and Technology, 39(7), 637-658, 2005.

Ebert, M., Weinbruch, S., Hoffmann, P., and Ortner, H. M. The chemical composition and complex refractive index of rural and urban influenced aerosols determined by individual particle analysis. Atmospheric Environment, 38(38),6531-6545, 2004.

Eggleton, R. A. (1991). Gladstone-Dale constants for the major elements in silicates: Coordination number, polarizability and the Lorentz-Lorenz relation.Canadian Mineralogist, 29, 525–32, 1991.

EPA, US. 40 CFR Parts 50, 51, 52, 53, and 58-National Ambient Air Quality Standards for Particulate Matter: Final Rule. Federal Register, 78:3086–3286, 2013.

Feinberg, S., Williams, R., Hagler, G. S. W., Rickard, J., Brown, R., Garver, D., Harshfield., G., Stauffer, P., Mattson., E., Judge, R., Garvey, S. Long-term evaluation of air sensor technology under ambient conditions in Denver, Colorado. Atmospheric Measurement Techniques Discussion, 2018.

GRIMM, A. T. G. C. M. Aerosol spectrometer and dust monitor, series 1.108 and 1.109; M_E_IAQ_1108-1109- Spec_v2p4, 2010.

Hand, J. L., Kreidenweis, S. M. A new method for retrieving particle refractive index and effective density from aerosol size distribution data. Aerosol Science and Technology, 36(10),1012-1026, 2002.

Hinds, W. C. Aerosol Technology: Properties, Behavior, and Measurement of Airborne Particles, 2nd Ed., New York: Wiley-Interscience, 1999.

Hogrefe, O., Drewnick, F., Lala, G. G., Schwab, J. J., and Demerjian, K. L. Development, Operation and Applications of an Aerosol Generation, Calibration and Research Facility Special Issue of Aerosol Science and Technology on Findings from the Fine Particulate Matter Supersites Program. Aerosol Science and Technology, 38(S1), 196-214, 2004.

Holstius, D. M., Pillarisetti, A., Smith, K. R., and Seto, E. Field Calibrations of a Low-Cost Aerosol Sensor at a Regulatory Monitoring Site in California. Atmos. Meas. Tech. 7, 1121-1131, 2014.

Jimenez, J. L., Jayne, J. T., Shi, Q., Kolb, C. E., Worsnop, D. R., Yourshaw I., Seinfeld J.H., et al. Ambient aerosol sampling using the aerodyne aerosol mass spectrometer. Journal of Geophysical Research: Atmospheres, 108(D7), 2003.

Landen, D. D., Wassell, J. T., McWilliams, L., and Patel, A. Coal Dust Exposure and Mortality from Ischemic Heart Disease Among a Cohort of U.S. Coal Miners. Am. J. Ind. Med., 54:727–733, 2011.

Le, G. E., Breysse, P. N., McDermott, A., Eftim, S. E., Geyh, A., Berman, J. D., and Curriero, F. C. Canadian forest fires and the effects of long-range transboundary air pollution on hospitalizations among the elderly. ISPRS International Journal of Geo-Information, 3(2), 713-731, 2014.

Lee, A. K. Y., Abbatt, J. P. D., Leaitch, W. R., Li, S. M., Sjostedt, S. J., Wentzell, J. J. B., Liggio, J., and Macdonald, A. M. Substantial secondary organic aerosol formation in a coniferous forest: observations of both day-and nighttime chemistry. Atmospheric Chemistry and Physics, 16(11), 6721-6733, 2016.

Li, J. Y., Biswas, P. Optical Characterization Studies of a Low-Cost Particle Sensor. Aerosol and Air Quality Research, 2017, 17(7), 1691-1704, 2017.

Mätzler, C. MATLAB Functions for Mie Scattering and Absorption. Research Report No. 2002-08, 2002.

McMurry, P.H. A review of atmospheric aerosol measurements, Atmos. Environ, 34, 1959-1999, 2000.

McNamara, M. L., Noonan, C. W., Ward, T. J. Correction factor for continuous monitoring of wood smoke fine particulate matter. Aerosol and air quality research, 11(3), 315, 2011.

Mamali, D., Marinou, E., Pikridas, M., Kottas, M., Binietoglou, I., Kokkalis, P., Tsekeri, A., Amiridis, V., Sciare, J., Keleshis, C., Engelmann, R., Ansmann, A., Russchenberg, H.W.J., and Biskos, G.. Vertical profiles of fine and coarse aerosol particles over Cyprus: Comparison between in-situ drone measurements and remote sensing observations[C]//EGU General Assembly Conference Abstracts. 2017, 19: 12966.

Mønster, J., Rosenørn, T., Svenningsson, B., Bilde, M. Evaporation of methyl-and dimethyl-substituted malonic, succinic, glutaric and adipic acid particles at ambient temperatures. Journal of aerosol science, 35(12), 1453-1465, 2004.

Seinfeld, J. H., Pandis, S. N. (2016). Atmospheric chemistry and physics: from air pollution to climate change, 3rd Ed. John Wiley and Sons, NJ, 2016.

Smith, A. The Scattering of Light by Non-spherical Particles: Second Year Report. 2009.

Sousan, S., Koehler, K., Thomas, G., Park, J. H., Hillman, M., Halterman, A., Peters, T. M. Inter-comparison of low-cost sensors for measuring the mass concentration of occupational aerosols. Aerosol Science and Technology, 50(5), 462-473, 2016a.

Sousan, S., Koehler, K., Hallett, L., and Peters, T. M. Evaluation of the Alphasense optical particle counter (OPC-N2) and the Grimm portable aerosol spectrometer (PAS-1.108). Aerosol Science and Technology, 50(12), 1352-1365, 2016b.

Sullivan, R. C., and Pryor, S. C. Quantifying spatiotemporal variability of fine particles in an urban environment using combined fixed and mobile measurements. Atmospheric Environment, 89, 664-671, 2014.

Sun, Y., Zhang, Q., Macdonald, A. M., Hayden, K., Li, S. M., Liggio, J., Liu, P. S. K., et al. Size-resolved aerosol chemistry on Whistler Mountain, Canada with a high-resolution aerosol mass spectrometer during INTEX-B. Atmospheric Chemistry and Physics, 9(9), 3095-3111, 2009.

Sun, Y. L., Zhang, Q., Schwab, J. J., Chen, W. N., Bae, M. S., Lin, Y. C., Hung H. M., Demerjian, K. L. A case study of aerosol processing and evolution in summer in New York City. Atmospheric Chemistry and Physics, 11(24), 12737-12750, 2011.

Sun, Y. L., Zhang, Q., Schwab, J. J., Chen, W. N., Bae, M. S., Hung, H. M., Lin, Y.-C., Ng, N. L., Jayne, J., Massoli, P., Williams, L. R., Demerjian, K. L., Williams, L. R. Characterization of near-highway submicron aerosols in New York City with a high-resolution aerosol mass spectrometer. Atmospheric Chemistry and Physics, 12(4), 2215-2227, 2012.

Thermo Fisher Scientific, Inc. MIE pDR-1500 Instruction Manual, Franklin, MA, 356-370, 2014.

TSI Inc. Operation and Service Manual, DustTrak DRX Aerosol Monitor, Revision E, P/N 6008408, 2017.

Wallace, L. A., Wheeler, A. J., Kearney, J., Van Ryswyk, K., You, H., Kulka, R. H., Rasmussen P. E., Brook, J. R., Xu, X. Validation of continuous particle monitors for personal, indoor, and outdoor exposures. Journal of Exposure Science and Environmental Epidemiology, 21(1), 49-64, 2011.

Wang, X., Chancellor, G., Evenstad, J., Farnsworth, J. E., Hase, A., Olson, G. M., Sreenath, A., and Agarwal, J. K. A novel optical instrument for estimating size segregated aerosol mass concentration in real time. Aerosol Science and Technology, 43(9), 939-950, 2009.

Wang, Y., Li, J., Jing, H., Zhang, Q., Jiang, J., and Biswas, P. Laboratory Evaluation and Calibration of Three Low-Cost Particle Sensors for Particulate Matter Measurement. Aerosol Sci. Technol., 49:1063–1077, 2015.

Wang, Z. C., Calderón, L., Patton, A. P., Sorensen Allacci, M., Senick, J., Wener, R., Andrews, C. J., and Mainelis, G. Comparison of real-time instruments and gravimetric method when measuring particulate matter in a residential building. Journal of the Air and Waste Management Association, 66(11), 1109-1120, 2016.

Weast, R. C., ed., Handbook of Chemistry and Physics, 57th edition, CRC Press, Cleveland, 1976.

Zhang, Q., Canagaratna, M. R., Jayne, J. T., Worsnop, D. R., and Jimenez, J. L. Time-and size-resolved chemical composition of submicron particles in Pittsburgh: Implications for aerosol sources and processes. Journal of Geophysical Research: Atmospheres, 2005, 110(D7), 2005.

Zhang, X., Kondragunta, S. Temporal and spatial variability in biomass burned areas across the USA derived from the GOES fire product. Remote Sensing of Environment, 112(6), 2886-2897, 2008.

**Table 1.** The scattering angles and light source wavelengths used in the DRX, PDR, and the OPC-N2, as well the approximate price of each sensor.

| Sensor | DRX | PDR | OPC-N2 |
|---|---|---|---|
| Wavelength (nm) | 655 | 880 | 658 |
| Scattering angle (°) | 90 | 60-80 | 30 |
| Price ($) | ~10,000 | ~5,000 | ~500 |

**Table 2.** Slopes of the regression lines obtained when plotting optically reported PM values (for DRX, PDR, and OPC-N2); and calculated Mie scatter flux (for DRX_RF and PDR_RF) for different PSL sizes versus the PM mass concentration measured by the TEOM.

| Vs TEOM | 90 nm | 173 nm | 304 nm | 490 nm | 1030 nm |
|---|---|---|---|---|---|
| DRX | 0.86 | 0.90 | 3.73 | 2.56 | 0.93 |
| PDR | 0.32 | 0.28 | 1.34 | 3.14 | 1.30 |
| OPC-N2 | N/A | N/A | N/A | 0.68 | 0.48 |
| RF results | | | | | |
| DRX_RF | 0.53 | 3.73 | 11.07 | 8.90 | 4.83 |
| PDR_RF | 0.09 | 0.63 | 2.92 | 5.30 | 3.70 |

**Table 3**. Ratios of mass concentration measured by optical instruments to reference instruments for the four compounds and groups listed in Table S1 (the median volume diameters are added below the name of different groups), as well as the refractive indices of each aerosol used in the Mie scattering calculations.

| Ratio (vs TEOM or SMPS) | $(NH_4)_2SO_4$ | $NaNO_3$ | sucrose | adipic acid* |
|---|---|---|---|---|
| Refractive indices (n) | 1.521/1.523/1.533 | 1.587/1.336 | 1.54/1.567/1.572 | 1.439 |

| | | | | | |
|---|---|---|---|---|---|
| Group 1<br>153 nm | DRX | 0.85 | 0.58 | 0.92 | 0.61 |
| | PDR-1500 | 0.32 | 0.21 | 0.32 | 0.24 |
| | OPC-N2 | 0.026 | 0.015 | 0.018 | 0.01 |
| Group 2<br>202 nm | DRX | 1.34 | 0.96 | 1.65 | 0.91 |
| | PDR-1500 | 0.66 | 0.40 | 0.61 | 0.39 |
| | OPC-N2 | 0.09 | 0.07 | 0.08 | 0.03 |
| Group 3<br>231 nm | DRX | 1.57 | 1.06 | 1.90 | 1.23 |
| | PDR-1500 | 0.88 | 0.62 | 1.08 | 0.62 |
| | OPC-N2 | 0.2 | 0.14 | 0.17 | 0.09 |

*SMPS was used as the reference measurement for adipic acid (see text).

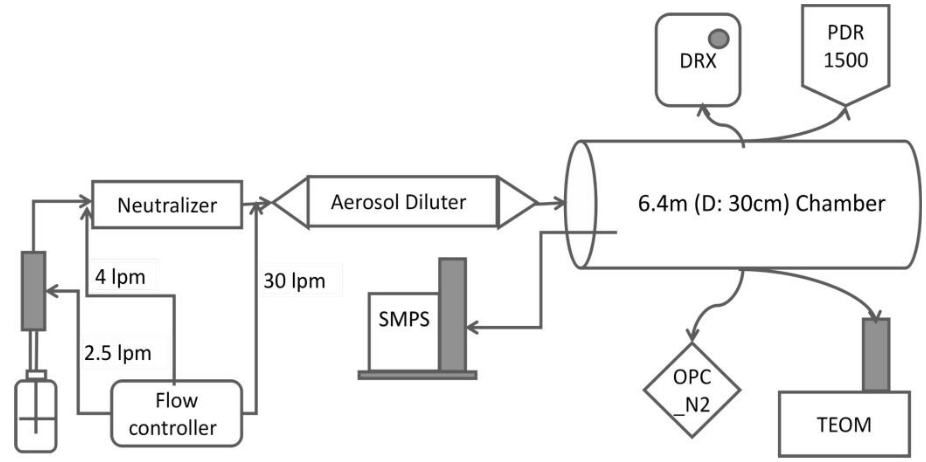

**Figure 1: Laboratory setup used for the evaluation and calibration of optical instruments using poly- and mono-disperse test aerosol**.

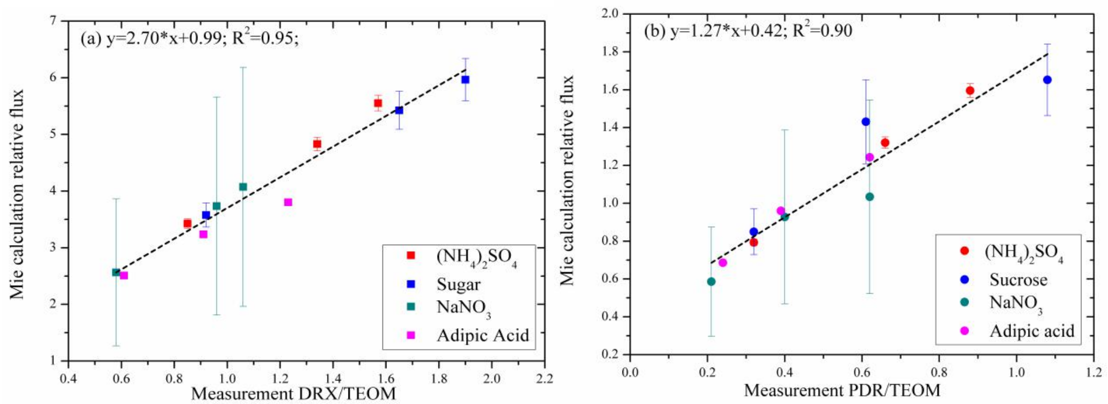

**Figure 2: The relationship of the Mie scattering relative flux and the measurement ratio of optical sensors to TEOM, (a) DRX; (b) PDR.**

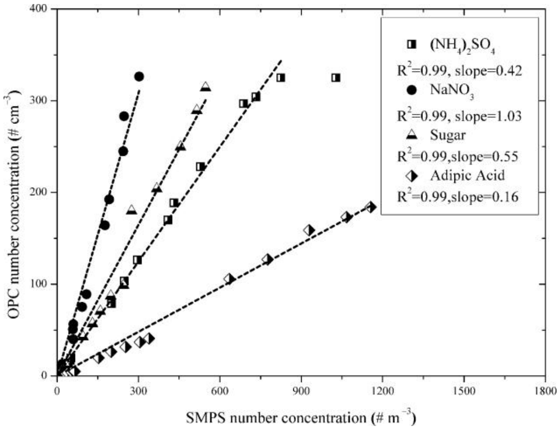

**Figure 3: The comparison of OPC and SMPS counts for four kinds of aerosol in the 380-540nm size range.**

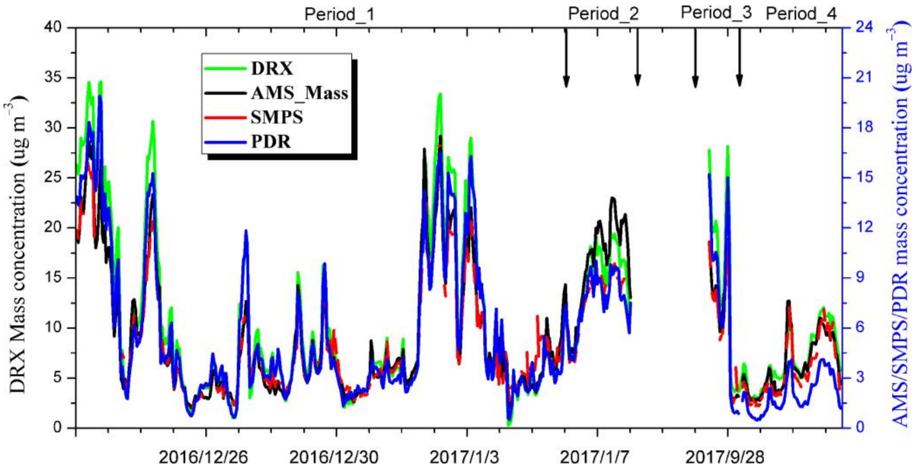

**Figure 4: The time series of 1-hour aerosol concentration measured by DRX, PDR, AMS, SMPS from 12/22/2016 to 01/07/2017 and 09/27/2017 to 10/01/2017.**

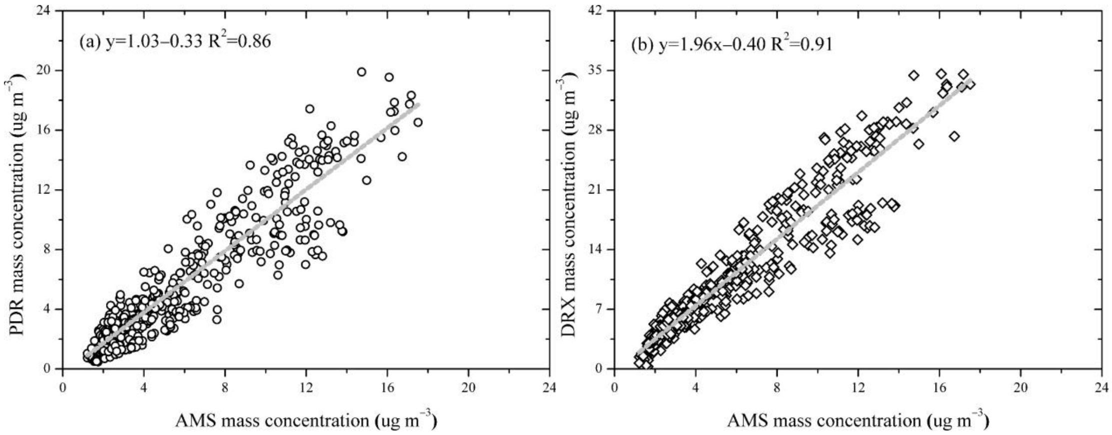

**Figure 5: The comparison of the 1-hr $PM_{2.5}$ average concentration between PDR (a) and DRX (b) observations with AMS measurements.**

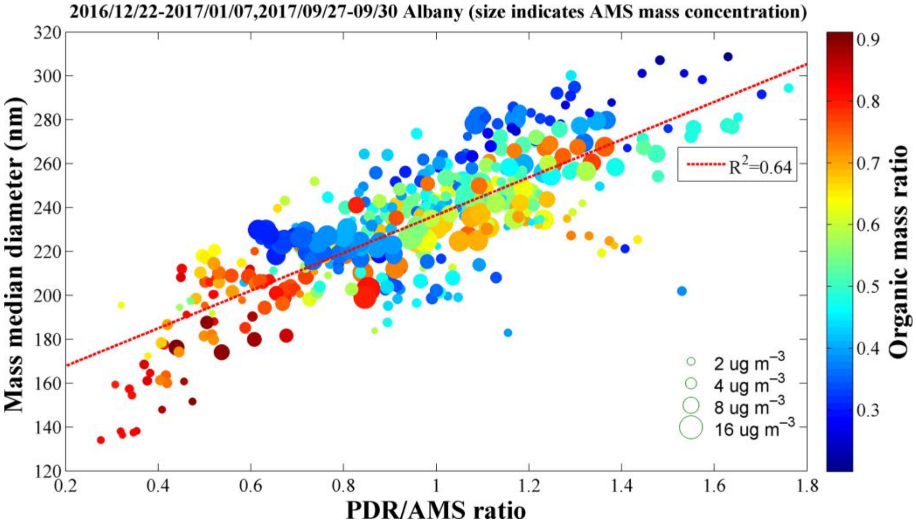

**Figure 6: The correlation scatterplot of aerosol median diameter and the PDR/AMS ratio. All points are colored by organic mass fraction, and sized by AMS mass concentration.**

Supplement Material for

# Exploring the Applicability and Limitations of Selected Optical Scattering Instruments for PM Mass Measurement

Jie Zhang*, Joseph P. Marto, James J. Schwab

Correspondence to：jzhang35@albany.edu

## S1 Estimation of aerosol density used for SMPS

The density of ambient aerosol was calculated based on organic, $SO_4$, $NO_3$, and $NH_4$ mass concentration measured by AMS (Zhang et al. 2005). It assumes that the organic composition had an averaged density of 1.20 g cm$^{-3}$, and that $SO_4$ and $NO_3$ were both components of salts, $(NH_4)_2SO_4$ (density 1.79g cm$^{-3}$) and $NH_4NO_3$ (density 1.72g cm$^{-3}$) respectively (Lee et al. 2015). The averaged ambient density was then calculated by:

$$\rho_{ambient} = \frac{m_{Total}}{\frac{m_{organic}}{\rho_{organic}} + \frac{m_{SO_4}}{\rho_{(NH_4)_2SO_4}} \times \frac{132}{96} + \frac{m_{NO_3}}{\rho_{NH_4NO_3}} \times \frac{80}{62}}$$

Where $\boldsymbol{\rho}$ is density, and $\boldsymbol{m}$ is the mass concentration.

## S2 Figures

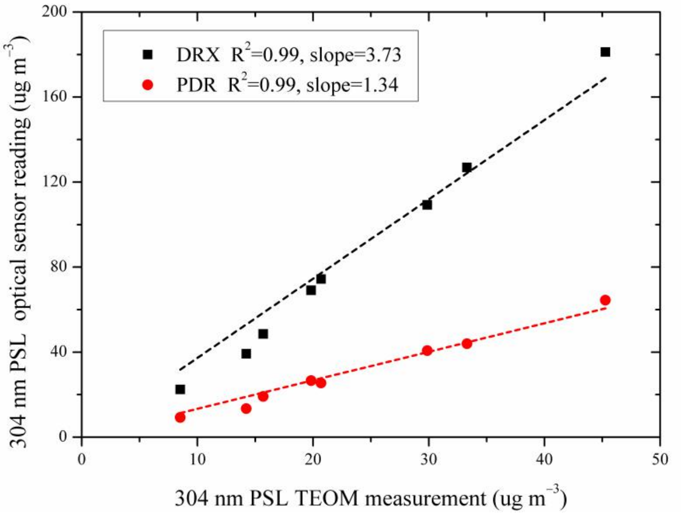

**Figure S1. The correlation between the reported mass concentration by optical sensors (DRX and PDR) and by TEOM.**

For this size PSL, the reading of OPC-N2 is not included. The OPC-N2 did not produce a response for the 304 nm and smaller PSL particles because of its 380 nm lower detection limit.

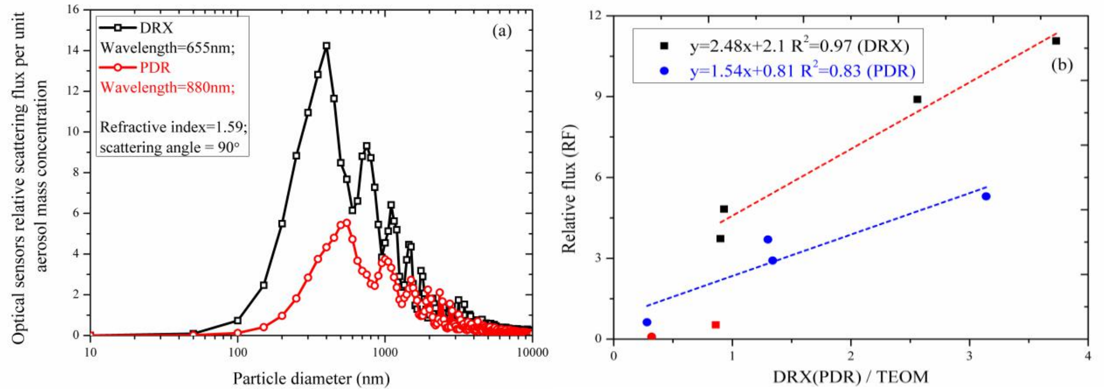

**Figure S2. (a) Results of a Mie scattering calculation for conditions appropriate to the DRX (black) and PDR (red); (b) Correlation between the relative flux with the ratio of optical instruments to TEOM (DRX: black; PDR: blue; and red points relates with the result of 90 nm PSL).**

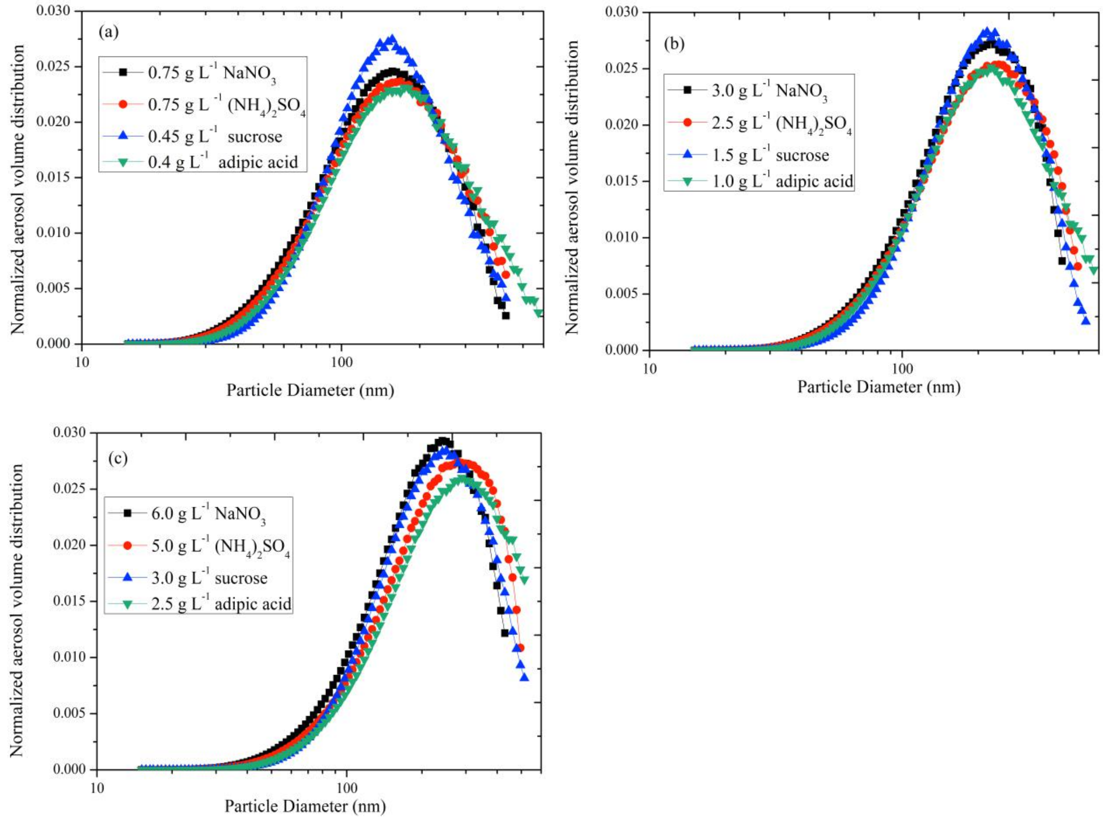

**Figure S3. The normalized volume distribution of three aerosol groups. (a) Group 1, with low concentration dilutions. (b) Group 2, with medium concentration dilutions. (c) Group 3, with high concentration dilutions.**

The volume concentration for each bin is divided by total integrated value for all bins to obtain normalized volume concentration in each bin, which shows the size distribution of different particles.

Figure S3 shows the shift in volume distributions for liquid samples with increasing concentration dilution. As the concentration increases, the volume distribution shifted rightward towards larger particles.

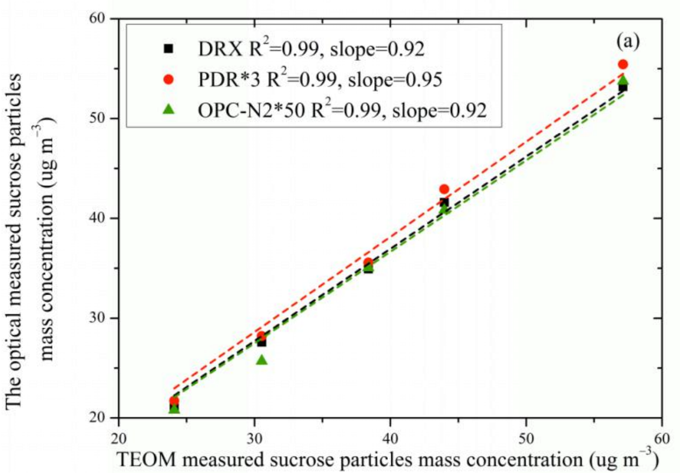

**Figure S4. Correlation between the readings of optical sensors and the reference TEOM measurement for 0.45 g $L^{-1}$ sucrose (For convenient comparison, PDR data is multiplied by 3, while OPC-N2 data s multiplied by 50).**

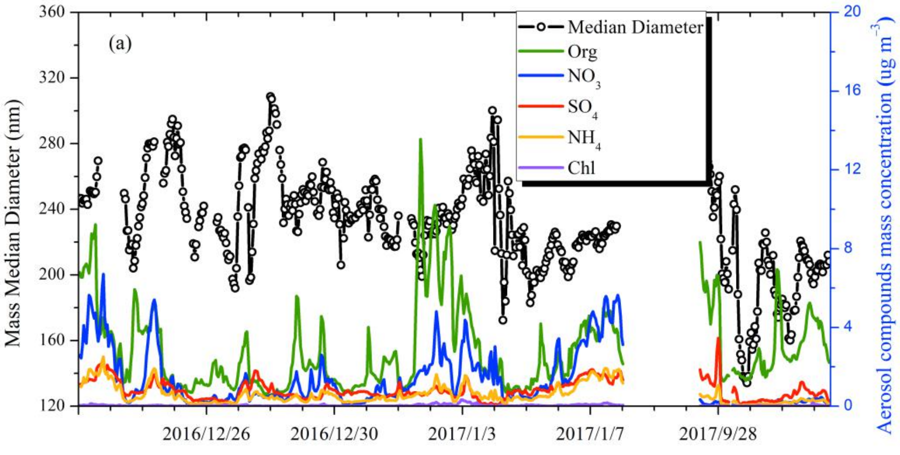

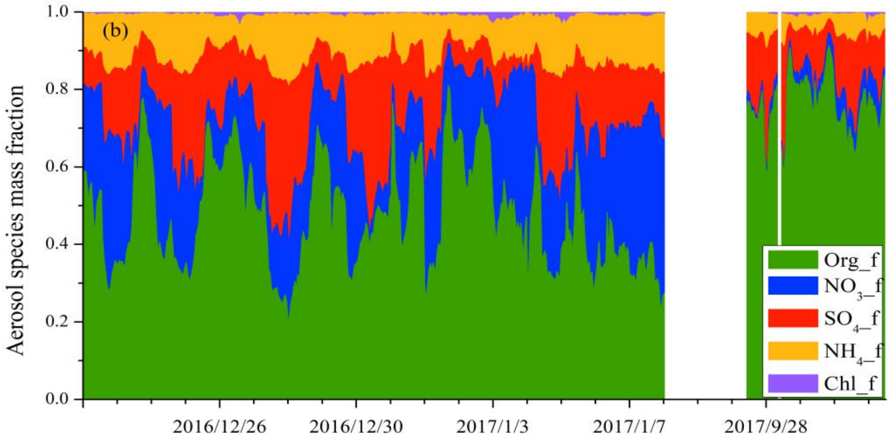

**Figure S5. (a) A time series of 1-hour aerosol composition concentration and SMPS mass median diameter. (b) The mass fraction of different chemical species in the composition from 12/22/2016 to 01/07/2017 and from 09/27/2017 to 10/01/2017.**

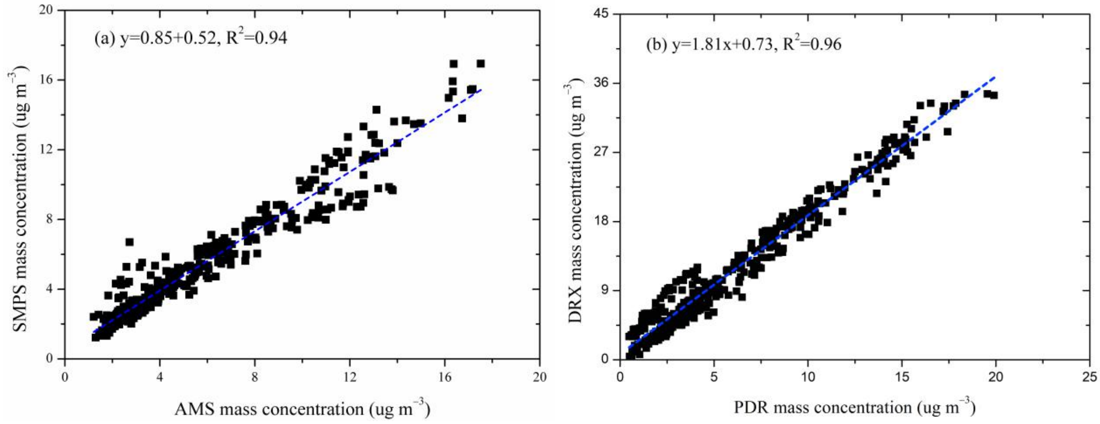

**Figure S6. (a) A scatterplot showing correlation of SMPS measurements to concurrent AMS measurements, and (b) correlation of DRX measurements to concurrent PDR measurements.**

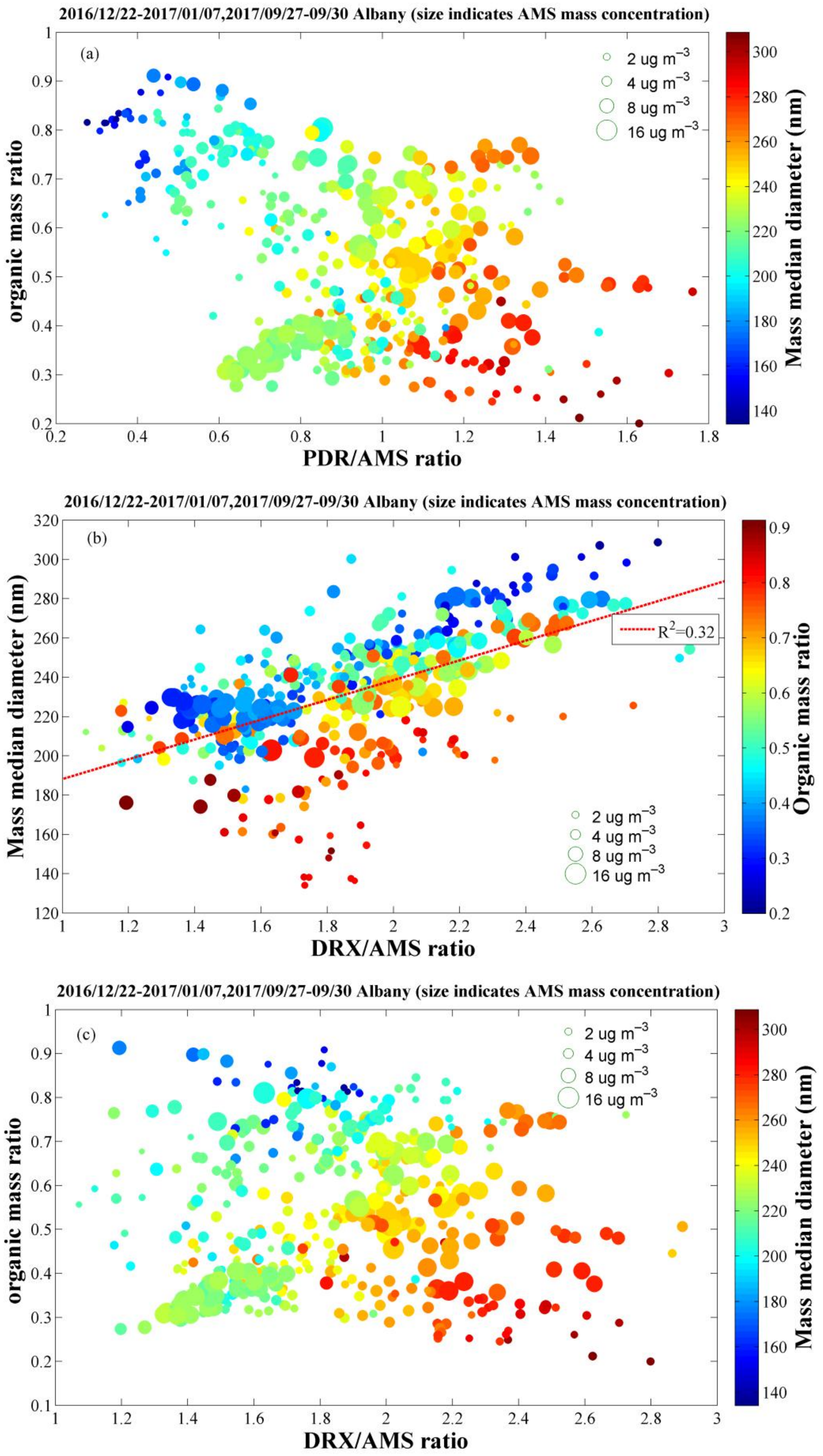

**Figure S7. (a) Scatterplot of organic mass fraction and the PDR/AMS ratio. Points are color-coded by aerosol median diameter. (b) Scatterplot and correlation of aerosol median diameter with the DRX/AMS ratio. Points are color-coded by organic mass fraction. (c)**

**Scatterplot of organic mass fraction with the DRX/AMS ratio. Points are color-coded by aerosol median diameter. Points are sized by AMS mass concentration.**

In Fig. S7b the correlation between aerosol median diameter with the DRX/AMS ratio was lower than with PDR/AMS, with the most deviated points the result of smaller diameter particles. One possible reason for the low correlation coefficient with DRX is that particles were with smaller size than other periods, and the aerosol with diameters smaller than 100 nm would cause significant bias to DRX, due to its size detection limit. After excluding the points with smaller size, the $r^2$ increases to 0.52, which demonstrates the positive effect of aerosol size on optical instrument response.

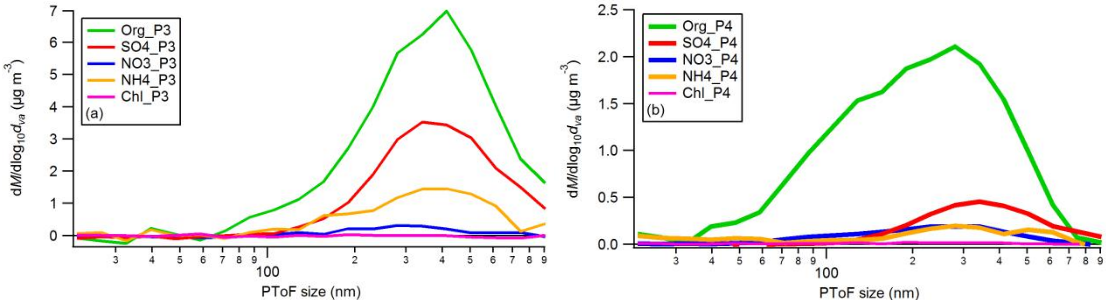

**Figure S8. (a) Averaged mass size distribution of long-distance transported aerosol composition, and (b) averaged mass size distribution of fresh aerosol composition.**

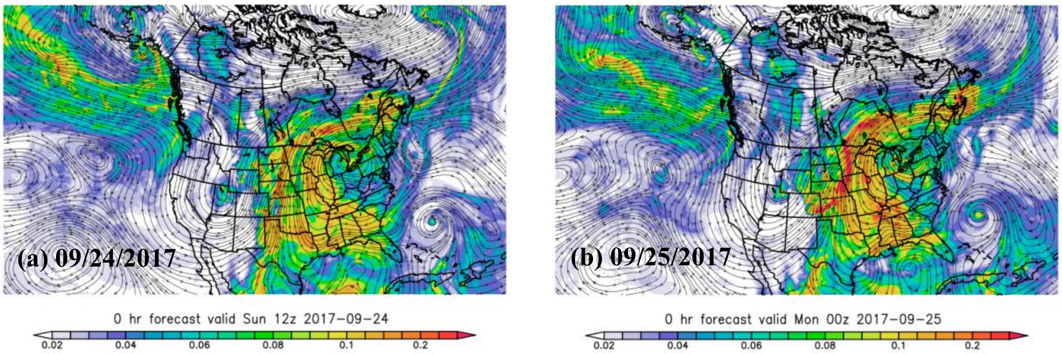

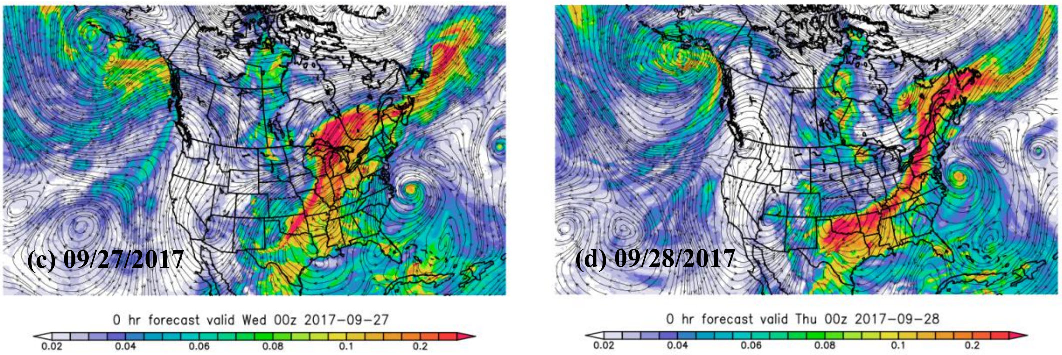

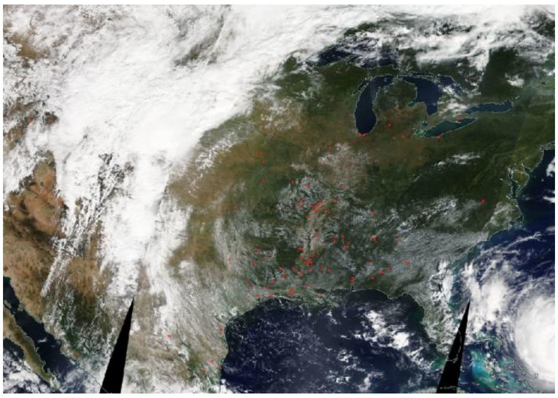

(e) the map of fires and thermal anomalies from Terra and MODIS

**Fig. S9. GEOS-5 forecasts for the spatial distribution of sulfate aerosol AOT over North America (https://portal.nccs.nasa.gov) on 09/24/2017, 09/25/2017, 09/27/2017, and 09/28/2017 (above four), and the map of fires and thermal anomalies from Terra and MODIS (https://worldview.earthdata.nasa.gov) on 09/23/2017**

It is believed that the sulfate aerosol originated from the lower Mississippi Valley on 09/24/2017, as a result of multiple point-source fires clustered in the region. As time progresses, the sulfate aerosol distribution changed with synoptic downstream flow, and created the prominent band that passes over New York State on 09/28/2017. During this process, the aerosol was believed to have experienced long-distance transport.

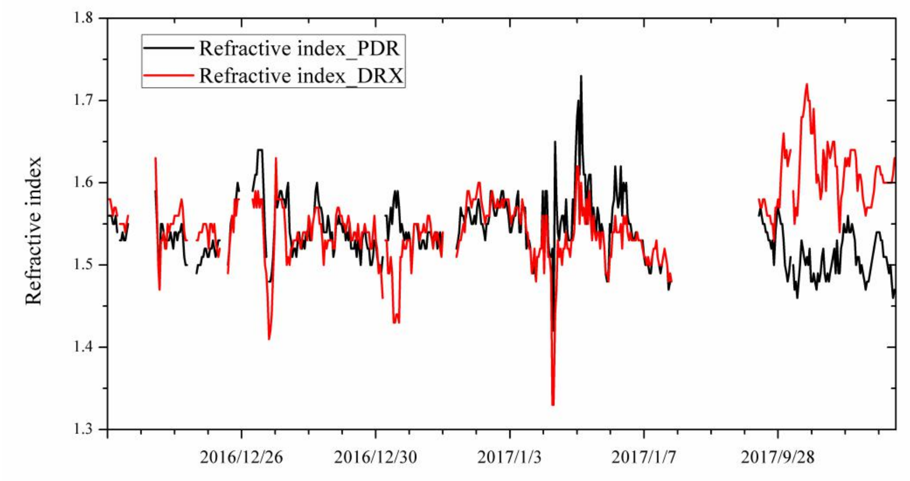

**Fig. S10. Time series of estimated aerosol refractive index estimated using the PDR and DRX.**

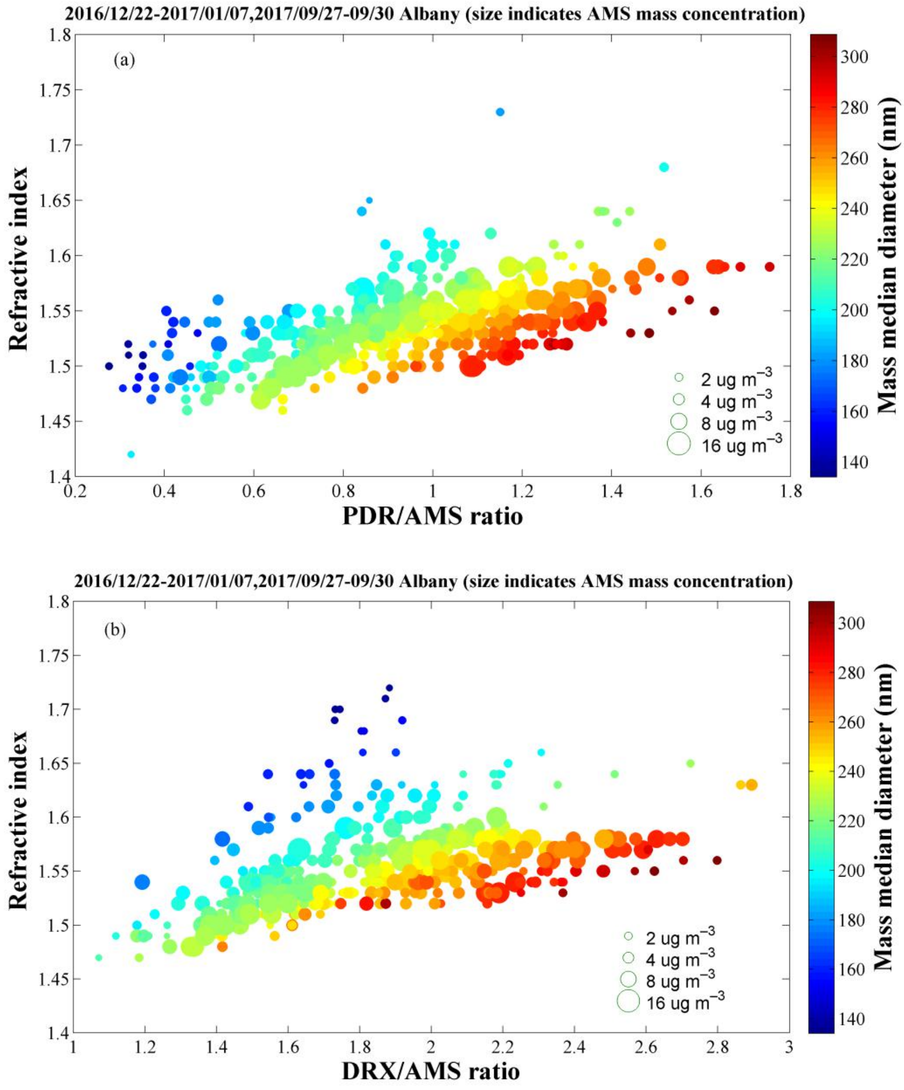

**Figure S11. (a) The correlation scatterplots of aerosol refractive index and the PDR/AMS ratio. (b) The correlation scatterplot of aerosol refractive index and the DRX/AMS ratio. All points are color-coded by aerosol median diameter, and sized by AMS mass concentration**

## S3 Tables

**Table S1. List of different dilution concentrations for each compound in the three test groups, and the volume median diameter of the generated size distribution.**

| Compound | Group 1 | Group 2 | Group 3 |
|---|---|---|---|
| $NaNO_3$ (g $L^{-1}$) | 0.75 | 3 | 6 |
| $(NH_4)_2SO_4$ (g $L^{-1}$) | 0.75 | 2.5 | 5 |
| Sucrose (g $L^{-1}$) | 0.45 | 1.5 | 3 |
| Adipic Acid (g $L^{-1}$) | 0.4 | 1.0 | 2.5 |
| Median Diameter (nm) | 153 | 202 | 231 |

**Table S2. Calculated relative Mie scattering flux of the four particle species (($(NH_4)_2SO_4$, $NaNO_3$, sucrose, adipic acid) analyzed by the PDR and DRX, and different dilution concentrations (#1 indicates Group 1; #2 indicates Group 2; #3 indicates Group 3).**

| Relative flux | $(NH_4)_2SO_4$ | $NaNO_3$ | sucrose | adipic acid |
|---|---|---|---|---|
| DRX(#1) | 3.37 | 2.56 | 3.34 | 2.50 |
| DRX(#2) | 4.72 | 5.04 | 5.04 | 3.19 |
| DRX(#3) | 5.41 | 5.54 | 5.54 | 3.72 |
| PDR(#1) | 0.79 | 0.59 | 0.86 | 0.69 |
| PDR(#2) | 1.31 | 0.93 | 1.45 | 0.96 |
| PDR(#3) | 1.59 | 1.03 | 1.67 | 1.24 |

**Table S3. Reference table RF for different refractive indices (TP refers to the time point for each hour of data, wavelength=880 nm, angle=90° )**

| Index/RF | TP1 | TP2 | TP3 | TP4 | TP5 | TP6 | TP7 | TP... |
|---|---|---|---|---|---|---|---|---|

| | | | | | | | | |
|---|---|---|---|---|---|---|---|---|
| 1.2 | 0.40 | 0.39 | 0.39 | 0.40 | 0.40 | 0.41 | 0.41 | ... |
| 1.21 | 0.45 | 0.43 | 0.43 | 0.44 | 0.44 | 0.45 | 0.45 | ... |
| 1.22 | 0.49 | 0.47 | 0.47 | 0.48 | 0.49 | 0.49 | 0.50 | ... |
| 1.23 | 0.53 | 0.52 | 0.51 | 0.52 | 0.53 | 0.54 | 0.54 | ... |
| 1.24 | 0.58 | 0.56 | 0.56 | 0.57 | 0.58 | 0.59 | 0.59 | ... |
| 1.25 | 0.63 | 0.61 | 0.61 | 0.62 | 0.63 | 0.64 | 0.64 | ... |
| ... | ... | ... | ... | ... | ... | ... | ... | ... |
| 1.75 | 6.04 | 5.85 | 5.73 | 5.91 | 6.01 | 6.06 | 6.11 | ... |
| 1.76 | 6.22 | 6.02 | 5.91 | 6.09 | 6.19 | 6.25 | 6.30 | ... |
| 1.77 | 6.41 | 6.21 | 6.08 | 6.28 | 6.37 | 6.43 | 6.49 | ... |
| 1.78 | 6.60 | 6.39 | 6.26 | 6.46 | 6.56 | 6.62 | 6.69 | ... |
| 1.79 | 6.79 | 6.58 | 6.45 | 6.65 | 6.75 | 6.82 | 6.88 | ... |
| 1.8 | 6.99 | 6.77 | 6.63 | 6.84 | 6.95 | 7.02 | 7.08 | ... |

**References:**

Zhang, Q., Canagaratna, M. R., Jayne, J. T., Worsnop, D. R., and Jimenez, J. L. Time-and size-resolved chemical composition of submicron particles in Pittsburgh: Implications for aerosol sources and processes. Journal of Geophysical Research: Atmospheres, 2005, 110(D7), 2005.

Lee, B. P., Li, Y. J., Flagan, R. C., Lo C., and Chan C. K.. Sizing characterization of the fast-mobility particle sizer (FMPS) against SMPS and HR-ToF-AMS. Aerosol science and technology, 47(9): 1030-1037, 2013.